JOURNAL OF MATERIALS SCIENCE 16 (1981) 1913–1924

The fracture of highly crosslinked polymers

Part 1 *Characterization and fracture toughness*

B. W. CHERRY, K. W. THOMSON
Department of Materials Engineering, Monash University, Clayton, Victoria, 3168, Australia

Five epoxy resin systems using plasticized and unplasticized resins have been characterized by conducting compression tests, modulus determinations and thermal analysis. The fracture toughness of these materials was then measured over a wide range of testing rates. Fracture was found to occur by slow stable, fast unstable or fast stable crack propagation and the type of behaviour could be correlated with the minimum post yield stress.

1. Introduction

Highly crosslinked polymers are finding an ever increasing range of applications as the matrix in fibre reinforced composites, as adhesives and as casting, coating and encapsulating materials. In general, their use in load bearing situations requires high strength and modulus. Attempts to attain these properties often result in a material with low fracture toughness. Additives such as plasticizers, reactive elastomers or fillers may be used to improve the toughness but will generally reduce the tensile strength, modulus and heat distortion tolerance. Thus, the brittleness of highly crosslinked polymers is a fundamental problem. From a design point of view, this problem is compounded by a large variation in reported values of toughness [1], conflicting results with regard to creep cracking behaviour [2–5], the dependence of toughness on crack velocity [1, 6–8] and the effect of hardener content [9–12] and other variables [13–15].

A further major problem is that crack propagation has been observed to proceed either in a continuous, stable manner or unstably, by a series of rapid jumps. Several studies [3, 5, 16, 17] have reported a transition from unstable to stable propagation with either increasing testing rate or decreasing temperature and this appears to be consistent with a crack blunting mechanism [18, 19]. A transition from stable to unstable propagation with increasing testing rate has, however, also been reported [20]. Furthermore, although the unstable to stable transition has been associated with a decrease in initiation toughness [3], another system showing a decrease in initiation toughness of almost a factor of ten showed no transition to stability [21].

Crack instability may be caused by a number of factors. If the specimen has a geometry such that the strain energy release rate (G) increases under the appropriate loading conditions as the crack grows, then it will tend to be unstable [22]. In this case dG/da is positive (a is the crack length). Alternatively, instability may result from a decreasing fracture surface energy (R), with increasing crack length as exemplified by environmental effects [23, 24]. In this case dR/da is negative. This would also occur if crack blunting was important, since a high toughness is recorded for the first increment of crack growth due to the low stress concentration ahead of the crack tip. A lower toughness is measured for the propagating crack. A further possibility is that the fracture surface energy may decrease with increasing crack velocity due, for example, to the effect of the temperature rise at the crack tip [25]. Here $dR/d\dot{a}$ is negative and the crack is again unstable. In the case of epoxy resins, specimens with stable geometries may still fracture unstably and there is evidence that environmental effects may be discounted [26]. Thus the fracture instability appears to be an inherent material property which requires further study.

0022–2461/81/071913–12$03.20/0 © *1981 Chapman and Hall Ltd.*

This paper reports on the first part of an investigation into the fracture behaviour of highly crosslinked polymers aimed at understanding the stability of fracture and developing a model capable of exhibiting most of the fracture phenomena which have been observed. Characterization of experimental materials and fracture toughness testing will be dealt with here. A subsequent paper will describe the detailed examination of the fracture surfaces which will allow further conclusions about the fracture behaviour to be made.

2. Materials

Epoxy resins were chosen as experimental materials because they are readily available, have low shrinkage which reduces problems of internal stress, have been widely used in previous studies and are of great commercial importance. A large range of bulk properties was required since this was expected to maximize the range of fracture properties exhibited and facilitate correlations between bulk and fracture properties. For this reason a plasticized and an unplasticized resin were chosen and these were cured with either a tertiary or mixed primary – secondary amine hardener.

Epikote 828, manufactured by Shell Chemical (Australia) Pty Ltd, was used for the unplasticized resin. It is an unmodified liquid resin with low molecular weight [27] and an epoxy molar mass average of 188. The plasticized resin was Araldite D (Ciba-Geigy Australia Ltd) which apparently contains about 23% plasticizer by weight implying an epoxy molar mass of approximately 244.

Triethylenetetramine (TETA) and tetraethylenepentamine (TEPA) were used as the mixed primary–secondary amine hardeners and triethylamine (TEA) was used as the tertiary amine hardener. TETA was obtained as a commercial hardening agent, HY951 (Ciba-Geigy) and TEPA and TETA were obtained as reagent grade chemicals. Details of the five systems investigated with hardener ratios and stoichiometric ratios are shown in Table I. Tertiary amines operate catalytically so no stoichiometric ratio can be calculated.

The resins and hardeners were weighed to an accuracy of ± 0.1 g to give batches of 80 to 90 g when mixed, so the hardener ratio could be controlled to an accuracy of ± 2% of the nominal value. The resin and hardener were mixed by hand for about 1 min which removed all visible inhomogeneities. Vacuum degassing for 15 min after mixing was used only for the D/TETA system. The 828 resin was heated to 70° C to lower its viscosity before mixing with the hardener and this allowed all the bubbles to rise quickly to the surface after pouring into silicon rubber moulds. Specimens were cast in blocks with approximate dimensions of 127 mm x 37 mm x 15 mm, from which fracture toughness, elastic modulus and plane strain compression specimens were machined. Uniaxial compression specimens were cast as cylinders using another set of moulds.

All curing schedules were carried out in air circulation ovens in which the temperature was controlled to ± 1° C. Curing temperatures were kept as low as possible to reduce residual stress. The curing schedules are given in Table I. The blocks produced all had a uniform colour and were free of bubbles. Examination in a polariscope showed that they contained only small amounts of residual stress.

A very low content of hardener was used for the 828/TETA system since very rapid curing, with a high exothermic energy, occurred for hardener ratios approaching stoichiometry. This resulted in a non-uniform solid with high internal stresses.

The nominal curing schedule for the D/TETA system was 30° C for 24 h. Some experiments were also carried out with specimens which had been postcured for 24 h at 70° C.

3. Characterization

3.1. Thermal analysis

Thermal analysis was used to determine the glass transition temperatures and to investigate the state of cure of the five epoxy systems. A Perkin–Elmer DSC-2 differential scanning calorimeter was used to obtain thermograms in the range 290 to 400 K from specimens with various curing schedules, and to obtain isothermal curves of heat input against time at the curing temperature.

TABLE I Experimental details

Material	phr	Stoichiometric ratio (phr)	Nominal curing schedule
D/TETA	10	10	30° C for 24 h
D/TEA	7.5	–	30° C for 24 h 50° C for 120 h
828/TETA	5	13	30° C for 24 h 70° C for 48 h
828/TEPA	10	14.5	30° C for 24 h 70° C for 24 h
828/TEA	7.5	–	30° C for 24 h 50° C for 120 h

The glass transition is associated with a shift in the specific heat which should appear as a step in the thermogram. In fact, due to thermal lags, an apparent endothermic peak is often observed. The glass transition temperature has been defined as being the point of onset of this peak which may overestimate the true glass transition temperature. Incomplete curing is indicated by the appearance of an exothermic peak when the scan temperature exceeds the glass transition temperature allowing the curing reaction to proceed [28]. Full details of this work will be reported elsewhere. Glass transition temperatures and states of cure are summarized in Table II. Full curing is assumed to occur when the exothermic peak becomes undetectable after the glass transition.

3.2. Elastic modulus

Third span, four point bend tests were selected to measure the elastic moduli of the epoxy systems. The specimens were milled to the dimensions 5 mm x 10 mm x 110 mm and tested in an instrument with a 90 mm span between the outer loading points. A testing rate of 0.05 cm min^{-1} was used and the modulus was calculated from the gradient of the load–deflection curve which was linear. The maximum stress was well below the yield stress and shear deflections were calculated to contribute less than 1% of the total deflection.

Two specimens from each system were tested and the spread in the results was comparable to the estimated uncertainty of the measurement (± 0.03 GPa). The average values are reported in Table II.

3.3. Yield behaviour

The yield behaviour of highly crosslinked polymers is dependent on the strain rate and on the state of stress. The stress–strain curve may or may not show a stress maximum followed by a strain softening stage [3, 29]. Previous workers [3, 18, 19] have found that fracture stability may be correlated with yield stress and hence the yield behaviour of the systems used in the present study was examined in some detail.

The brittle nature of epoxy resins necessitates the use of compression rather than tensile testing. This may introduce problems in applying compressive yield data to the tensile yielding situation encountered during fracture. As a first approach to this problem, yield data was obtained from two compressive stress systems; plane strain and uniaxial, and will be discussed in terms of a yield criterion. Tests were carried out over two decades of strain rate and yield points are defined in the inset to Fig. 1.

Specimens for plane strain compression tests [30] were milled from cast blocks to a thickness of 5 mm and width 30 mm. They were compressed between 12.7 mm thick dies lubricated with molybdenum disulphide grease and equipped with displacement transducers to drive one axis of an $X-Y$ recorder. The second axis of the recorder

TABLE II Bulk properties

Material	T_g*	State of cure	Young's modulus (GPa)
D/TETA	50	Undercured	2.92
D/TEA	63	Fully cured	2.12
828/TETA	54	Undercured	3.81
828/TEPA	84	Undercured	3.76
828/TEA	80	Undercured	3.37

*Extrapolated onset temperature of endothermic peak in thermogram.

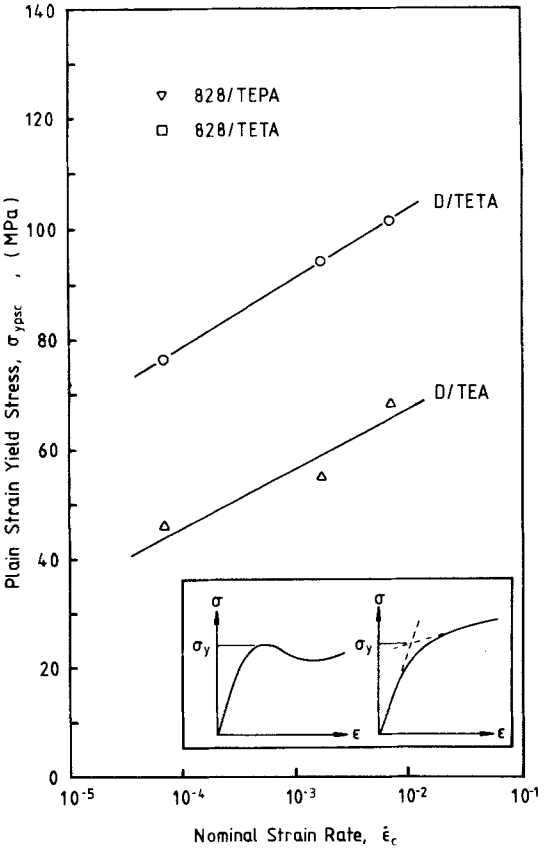

Figure 1 Plane strain compression yield stress, variation with nominal strain rate.

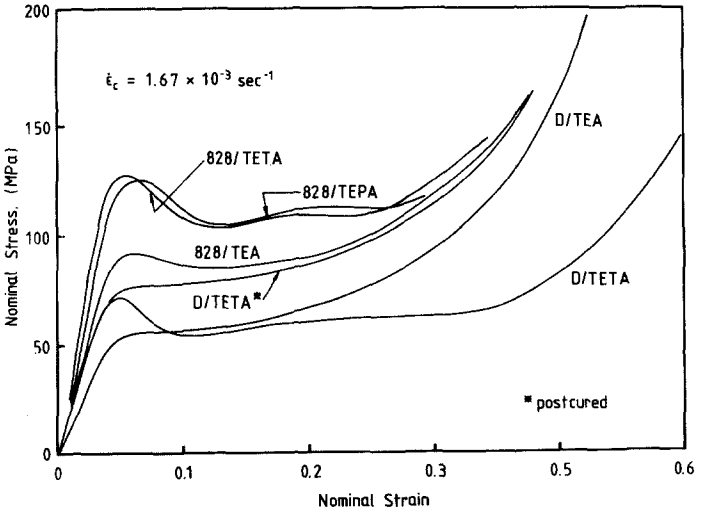

Figure 2 Uniaxial compression curves.

was driven by the output of the testing machine's load cell. The yield stress was calculated from the nominal contact area of the dies (12.7 mm x 30 mm) and a nominal value of strain rate was calculated from the initial specimen thickness and the crosshead speed of the testing machine.

Uniaxial compression specimens were cast cylinders about 12.5 mm in diameter with machined end faces. They were compressed between platens lubricated with teflon sheet and molybdenum disulphide grease. Photographs of the specimen were taken during each test and these showed that uniform deformation, with a maximum variation in diameter of 1%, occurred up to the stress maximum. The photographs were used to calculate the end face area at the yield point. Although buckling and bollarding often occurred after yield, approximate values for the minimum stress after the yield point were also calculated using the end face area at the yield point and the minimum post-yield load.

The plane strain compression data was limited by the tendency for fracture to occur in the region between the compressed and uncompressed parts of the specimen. This caused loss of constraint and changes to the stress system. The general form of the stress–strain curves was the same for plane strain and uniaxial compression; curves for uniaxial compression at one strain rate are shown in Fig. 2. Plane strain compression yield data is plotted in Fig. 1 and uniaxial data in Fig. 3. Post-yield minimum stress is plotted in Fig. 4 and is recorded as identical to the uniaxial yield stress in cases where no post-yield minimum occurred.

4. Fracture toughness tests

4.1. Experimental procedure

Important considerations in the selection of a specimen geometry for this investigation were a sufficiently negative geometrical stability factor

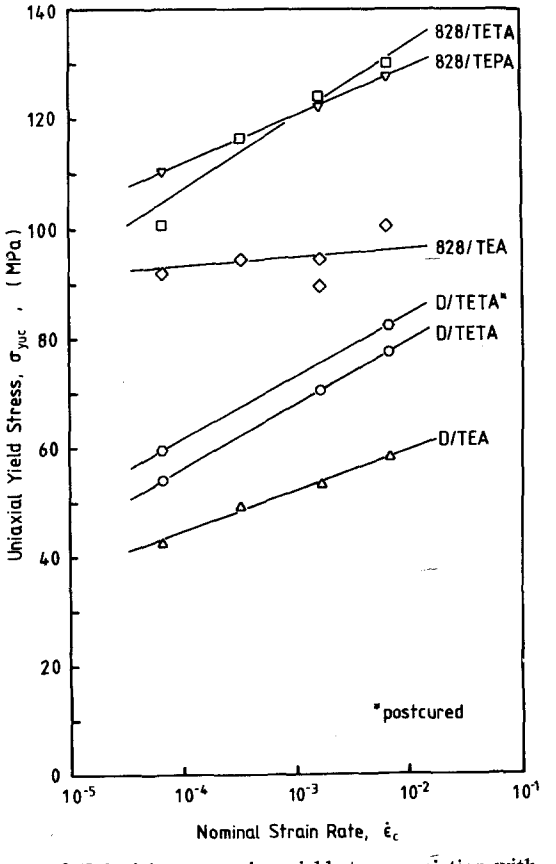

Figure 3 Uniaxial compression yield stress, variation with nominal strain rate.

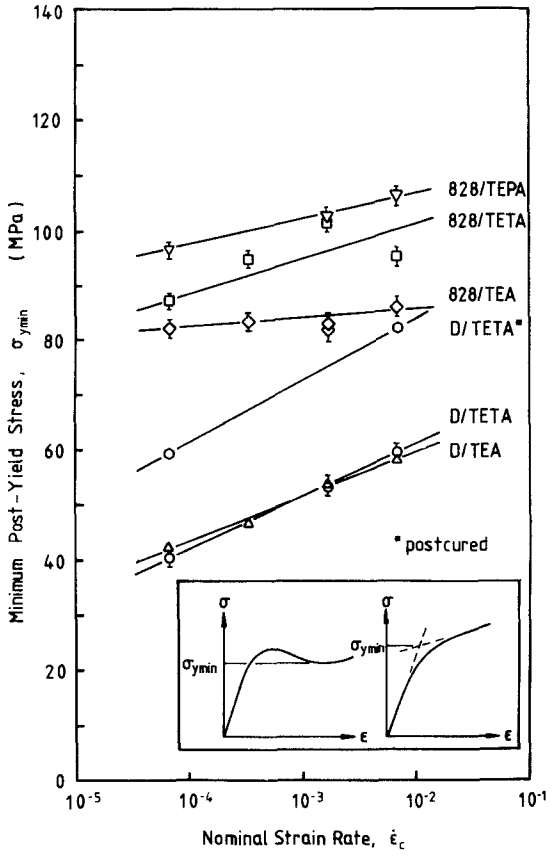

Figure 4 Minimum post-yield stress, variation with nominal strain rate.

[22], control of the crack direction and the ability to form a reproducible precrack. The geometrical stability of tapered double cantilever beam specimens increases as the taper angle decreases [6] and is greatest for a parallel sided double cantilever beam (although further improvement can be obtained by reversing the taper angle). Double torsion specimens have been widely used in the past and have produced excellent results [5, 14, 16]. However, the geometric stability of a double torsion specimen is not as great as the parallel sided double cantilever beam. Furthermore, the crack front is curved with double torsion specimens which may introduce a variety of complications [31]. For these reasons a parallel sided double cantilever beam specimen, with deep side grooves for control of the crack direction, was selected (Fig. 5).

Precracking was performed by sharpening an initial saw cut with a razor blade and then loading with a load-point displacement rate of 0.05 cm min^{-1} until a crack propagated unstably

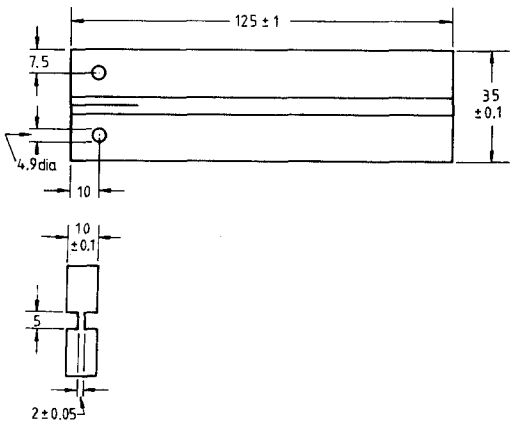

Figure 5 Double cantilever beam specimen (dimensions in mm).

and arrested between 25 and 80 mm from the line of action of the loading points. This natural precrack was then used for the actual experiment. When unstable crack growth occurred, successive measurements could be taken from the same specimen in some cases.

Toughness was calculated using the equation,

$$G = \frac{1}{2b} P^2 \frac{dC}{da} \quad (1)$$

where P is the load, b is the specimen width in the fracture plane, a is the crack length and C is compliance. An expression for the dC/da term was obtained from an experimental compliance calibration derived for a specimen of each material. Additional experiments were carried out to measure toughness and crack velocity as a function of crack length during slow crack propagation. The crack tip was located by photographing the crack tip region.

Some experiments with single edge notched specimens were performed to examine the effect of specimen thickness and postcuring on crack propagation in D/TETA. These specimens were made from cast sheet 2 or 4 mm thick, 35 mm wide and 120 mm long. They were precracked by tapping a razor blade into the end of an initial sawcut while the specimen was lightly compressed in a vice. This caused the crack to jump a few millimeters and then arrest to form a natural precrack.

4.2. Results

Four types of fracture behaviour could be identified according to the shape of the load–load-point

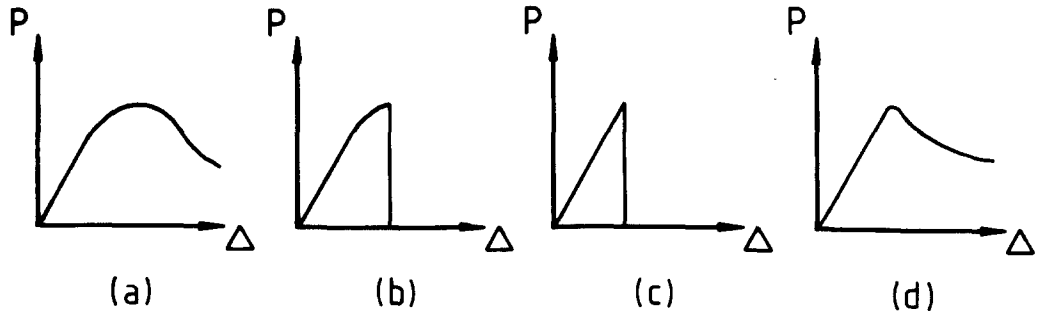

Figure 6 Load–load-point displacement curves defining (a) Type IA, (b) Type IB, (c) Type II, and (d) Type III fracture behaviour.

displacement curve (Fig. 6). In some systems at very slow testing rates, some stable crack extension was observed. This is characterized by a loading curve with a decreasing gradient which may either become negative as the crack extends stably for a considerable distance along the specimen (type IA) or drop suddenly when the crack becomes unstable (type IB). Type II crack growth is defined by a loading curve with no detectable decrease in gradient before the maximum load, at which point the crack propagates unstably causing a rapid load drop. Type III crack growth may occur at faster testing rates by stable crack growth from the pre-crack. The load drops gradually from the maximum as the crack propagates along the specimen. No significant decrease in gradient is observed before the maximum load is reached.

The location of the transitions in fracture behaviour could only be defined within about half a decade of the load-point displacement rate. Some variation in behaviour may be due to the effect of crack length on the strain rate experienced by material near the crack tip.

The results for the D/TETA system (Fig. 7) showed type IA fracture at testing rates up to about 2×10^{-2} cm min^{-1}. Observation of the crack tip with a microscope during loading showed that the crack initiated at a comparatively low load and that this coincided with the point at which the loading curve deviated from linearity. The load then increased to a maximum value as the crack continued to extend. Two toughness values could be defined; the initiation toughness, G_i, calculated from the load when the first crack extension was observed, and a maximum toughness, G_{max}, calculated from the maximum load. The length of the precrack measured on the fracture surface was used to calculate both values of the toughness and hence G_{max} is an underestimate of the true toughness. G_i values are shown by upward facing arrows in Fig. 7 and the points are numbered so that corresponding G_i and G_{max} values can be identified.

At faster testing rates the crack became unstable after only limited crack growth producing type IB loading curves. Above a load-point displacement rate of about 10^{-1} cm min^{-1}, type II behaviour was obtained and G_i was coincident with G_{max}. This behaviour persisted at the highest testing rates used (10^2 cm min^{-1}). The maximum toughness values for type I fracture were more than an order of magnitude higher than the toughness for type II behaviour.

Fig. 8 shows the results for the 828/TETA system. There is some evidence for increasing toughness at very slow testing rates and there is a change in fracture behaviour at a load-point displacement rate of about 1 cm min^{-1} from type II to type III. The toughness for type III fracture does not appear to be lower than for type II behaviour. The results of 828/TEPA (Fig. 9) are very similar although the type II and type III transition occurs at a load-point displacement rate which is about one decade slower.

The fracture toughness of the D/TEA system (Fig. 10) is higher than that of all other systems except D/TETA. Again there is some evidence of the toughness increasing at very low load-point displacement rates. A transition from type IB to type II behaviour occurs at a load-point displacement rate of about 5×10^{-3} cm min^{-1}. 828/TEA has the lowest toughness of all the systems tested (Fig. 11) and type II behaviour was observed over the entire range of testing rates.

Crack velocity and fracture toughness measured as a function of crack length for type I crack growth in D/TETA are plotted in Fig. 12.

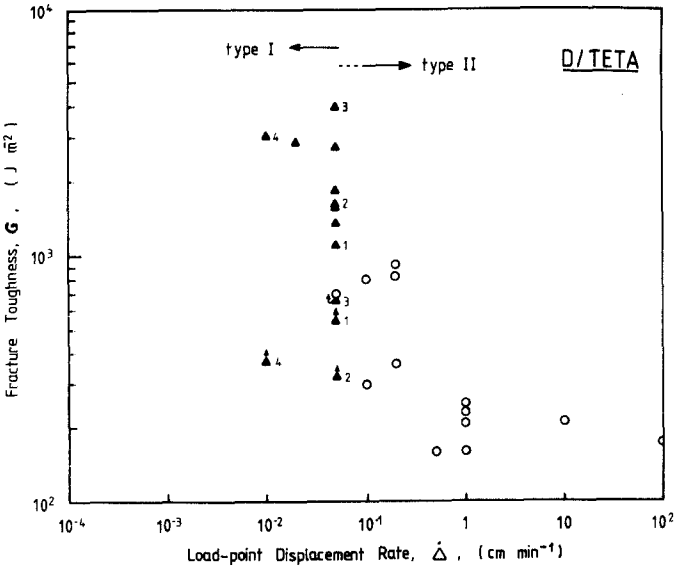

Figure 7 D/TETA fracture toughness, variation with testing rate.

The true crack length, measured from photographs taken during the test, was used to calculate toughness in this case.

Type I crack growth could also be obtained in 2 mm single edge-notched D/TETA specimens providing the displacement rate was 10^{-1} cm min^{-1} or less. At faster testing rates, type II behaviour was observed. When 4 mm thick specimens were used, however, type I crack growth could only be observed for load-point displacement rates less than 10^{-2} cm min^{-1}. Type I fracture could not be observed even at the slowest load-point displacement rates used (5×10^{-3} cm min^{-1}) with 2 mm thick specimens which had been postcured at 70° C for 24 h.

5. Discussion

5.1. Bulk properties

Despite the below stoichiometric hardener ratios and relatively low curing temperatures used for several of the systems, their yield stress and moduli were comparable to stoichiometric systems cured at high temperatures. This is particularly noticeable for the 828/TETA system which achieves high modulus and yield stress with only 5 phr hardener. The Araldite D based systems have lower yield stress and modulus values as would be expected because of the plasticizer. These results emphasize that exact stoichiometry is not essential in maximizing the bulk properties, a point that has been noted previously [9].

The uniaxial and plane strain compression yield points and the post-yield minimum stress generally show an increasing trend with strain rate which can be fitted reasonably well with a straight line when stress is plotted against the logarithm of the strain rate. 828/TEA is exceptional and appears to be comparatively strain rate independent.

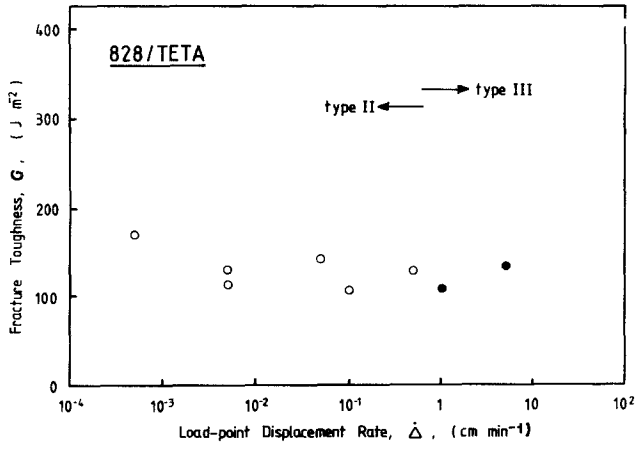

Figure 8 828/TETA fracture toughness, variation with testing rate.

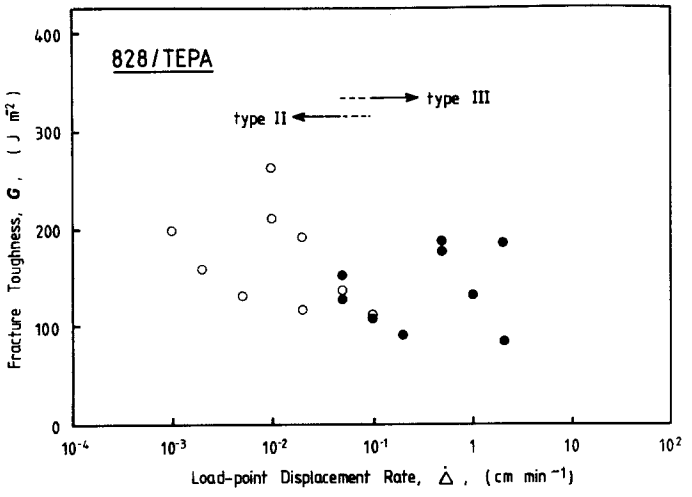

Figure 9 828/TEPA fracture toughness, variation with testing rate.

Previously [29, 32], modified von Mises yield criteria have been suggested for polymers. The yield data was analysed using the crtierion,

$$(\sigma_1 - \sigma_2)^2 + (\sigma_2 - \sigma_3)^2 + (\sigma_3 - \sigma_1)^2 = 6[K - \alpha(\sigma_1 + \sigma_2 + \sigma_3)]^2 \quad (2)$$

which reduces to the standard von Mises criterion when α is zero. Hence α may be used as a measure of the hydrostatic pressure dependence which becomes stronger as α becomes more positive. The stress system for plane strain compression is [29] $\sigma_1 = -\sigma$, $\sigma_2 = -\sigma/2$ and $\sigma_3 = 0$, and so substituting in Equation 2 for the plane strain compression yield point, σ_{ypsc}

$$\sigma_{ypsc} = 2\left(K + \frac{3\alpha\sigma_{ypsc}}{2}\right). \quad (3)$$

Similarly for uniaxial compression where $\sigma_1 = -\sigma$, and $\sigma_2 = \sigma_3 = 0$, the uniaxial compression yield stress is,

$$\sigma_{yuc} = 3^{1/2}(K + \alpha\sigma_{yuc}). \quad (4)$$

Equations 3 and 4 may be solved simultaneously to give values of K and α for the compression data where both σ_{yuc} and σ_{ypsc} are available. The results of this analysis are given in Table III. There is a large uncertainty in these values because of the scatter in the yield data. Negative values for α are unexpected and indicate inaccuracies in the measurements. However, from these preliminary results there does appear to be some evidence that yielding in D/TETA is fairly strongly dependent on hydrostatic pressure whereas in the other materials it is less so. The yield point in tension for D/TETA is then expected to be less than the compressive yield point.

5.2. Fracture behaviour

Three major types of fracture behaviour have been identified. These are: slow, stable fracture which

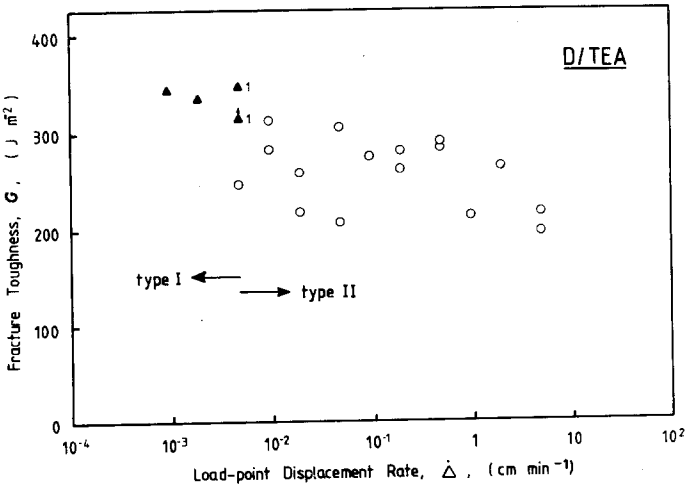

Figure 10 D/TEA fracture toughness, variation with testing rate.

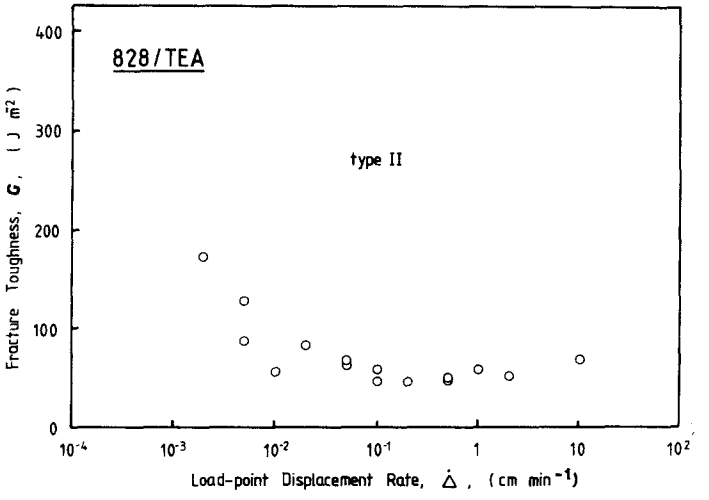

Figure 11 828/TEA fracture toughness, variation with testing rate.

may either remain stable for crack extensions of many millimeters (type IA) or become unstable after a short extension (type IB); fast, unstable fracture (type II) where there is no evidence of stable growth from the loading curve; and fast stable fracture (type III). The range of testing rates which produce each type of fracture behaviour are summarized in Fig. 13.

There have previously been some reports of slow stable fracture behaviour over a limited range preceding unstable fracture both in polyester resins [33] and epoxies [5, 19]. Kinloch and Williams [18] have called this type of fracture "ductile tearing". The existence of slow stable fracture suggests that some subcritical crack growth may be a general phenomenon. This may create complications with the crack blunting theory which assumes that the crack tip remains stationary during loading until a critical condition is reached in the region of the blunted crack tip at the maximum toughness.

There is some correlation between the low glass transition temperature of the plasticized resins and type I crack growth, and with the high glass transition temperature and type II or III behaviour of 828/TEPA and 828/TEA. 828/TETA, however, is an obvious exception in that it has a very low glass transition temperature but displays fracture behaviour similar to 828/TEPA.

Examination of the yield stress data shows that there is some correlation with fracture behaviour. Type I fracture is observed in the systems which have the lowest yield stress (D/TETA and D/TEA) and type III fracture is observed in systems with high yield stress (828/TETA and 828/TEPA). This correlation, however, is not particularly good because D/TETA has a higher yield stress than D/TEA but displays fully stable type IA crack

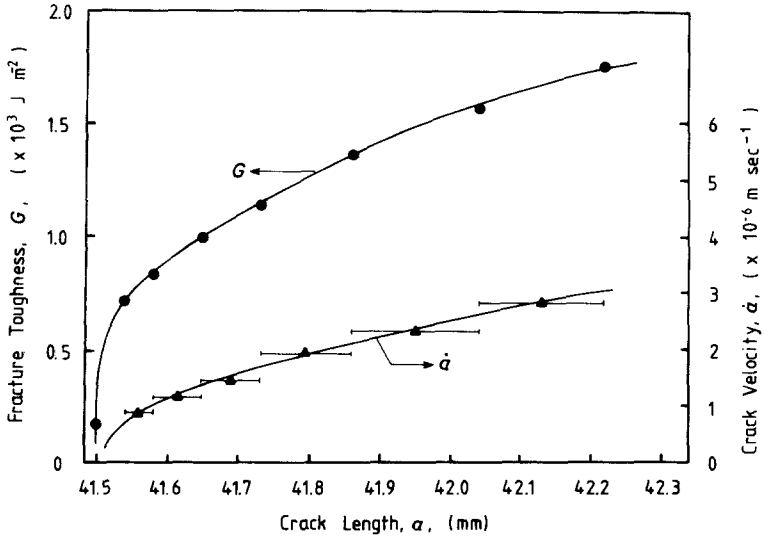

Figure 12 D/TETA fracture toughness and crack velocity, variation with crack length.

TABLE III Yield stress parameters

Material	$\dot{\epsilon}_{comp}$	σ_{ypsc}	σ_{yuc}	K	α
D/TETA	6.67×10^{-5}	76.7	54.0	24.8	0.12
	1.67×10^{-3}	94.1	70.6	34.5	0.09
	6.67×10^{-3}	101.5	78.7	39.8	0.07
D/TEA	6.67×10^{-5}	46.5	42.4	26.4	−0.05
	1.67×10^{-3}	55.2	53.4	36.7	−0.11
	6.67×10^{-3}	68.9	58.4	32.8	0.02
828/TETA	6.67×10^{-5}	118.2	108.1	67.6	−0.05
828/TEPA	6.67×10^{-5}	124.6	110.2	65.5	−0.02

growth at slow testing rates whereas D/TEA does not. Furthermore, 828/TETA and 828/TEPA have very similar yield stresses but the transition to type III behaviour occurs at a load-point displacement rate one order of magnitude slower than for 828/TETA.

Postcuring D/TETA was found to suppress type I crack growth although the effect on yield stress was small (Fig. 2). However, postcuring drastically changed the shape of the compression stress–strain curve by eliminating the post-yield minimum. This suggests that the minimum post-yield stress may be a better parameter for examining correlations with fracture behaviour than yield stress. This is reasonable since the minimum post-yield stress is probably more representative of the stress in the plastic zone than the yield stress.

It is then feasible to suggest that each type of fracture behaviour may be assigned to a range of minimum post-yield stress and that stability transitions may correlate with changes in minimum post-yield stress from one range to another as a result of changes in strain rate. To test this hypothesis a correspondence between the strain rates at which the yield point was determined in compression tests and load-point displacement rates in fracture tests is necessary.

For a stationary crack, Irwin [34] has shown that the rate of change in the tensile stress experienced at a point on the end of the yielded zone ahead of a crack tip may be approximated by

$$\dot{\sigma} = \frac{2\sigma_y}{t} \tag{5}$$

where σ_y is the yield stress and t is the time elapsed from the start of monotonic loading to yield. The strain rate experienced by material at

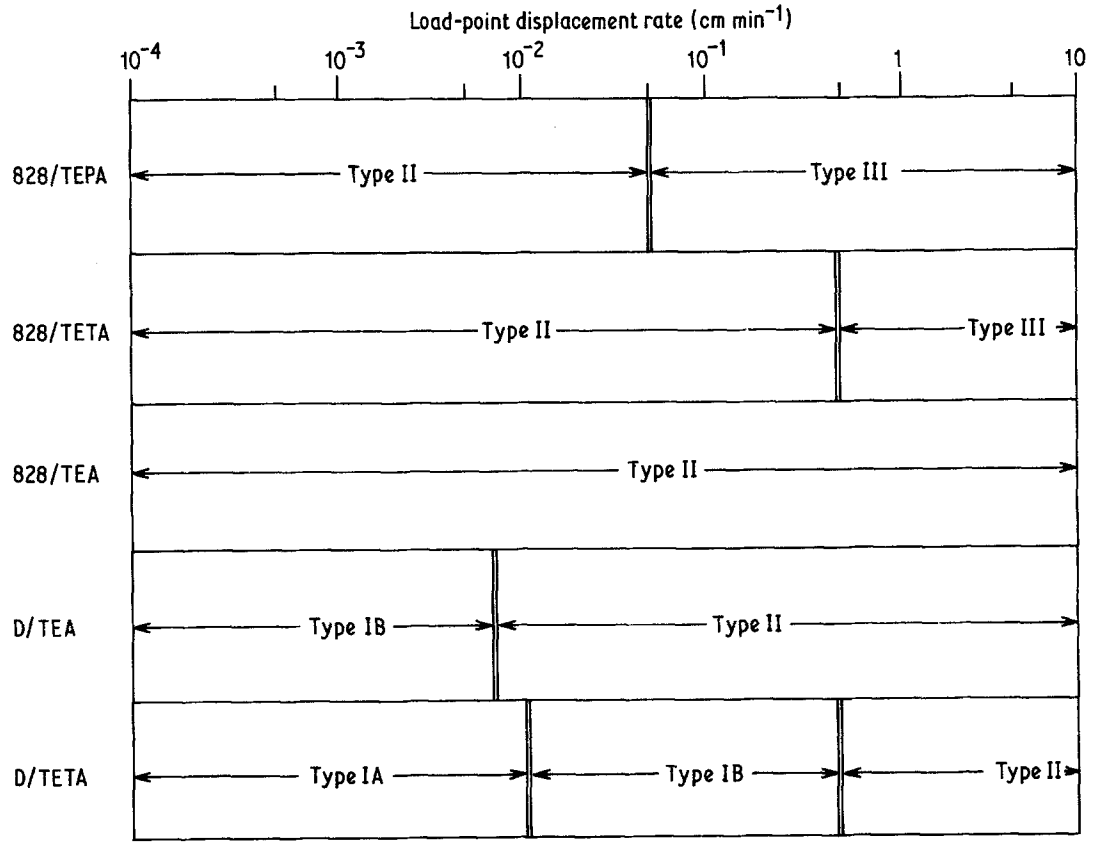

Figure 13 Summary of fracture behaviour.

the end of the yielded zone at the time of crack initiation may then be calculated from

$$\dot{\epsilon} = \frac{2\sigma_y}{Et} \quad (6)$$

where t is now the time at which the crack begins to extend. Substituting some representative values into this equation suggests that a reasonable relationship between the strain rate in a compression test ($\dot{\epsilon}_c$) and the load-point displacement rate ($\dot{\Delta}$ in cm min^{-1}) for a fracture test, which corresponds to equivalent strain rates at the end of the yielded zone is

$$\dot{\epsilon}_c = 6.7 \times 10^{-3} \dot{\Delta}. \quad (7)$$

Errors in the value of the constant will be shown to be of minor importance.

Minimum post-yield stress has been plotted as a function of testing rate in Fig. 14 using Equation 7. The regions of different fracture behaviour are indicated by the form of the extrapolated best fit line. Four regions of minimum post-yield stress can then be defined which correspond very well to the observed fracture behaviour. The correlation would be improved if the D/TETA line were lower than the D/TEA line since the former system shows fully stable type IA behaviour whereas D/TEA does not. As shown in the discussion of the yield stress data, there is some evidence that yielding should in fact occur at lower stress levels in D/TETA when tested in tension compared with its behaviour in compression.

The type II to type III transition occurs at 100 ± 5 MPa, the type IB to II transition at 55 ± 5 MPa and the type IA to IB transition at about 45 MPa. Errors in the relationship between $\dot{\epsilon}_c$ and $\dot{\Delta}$ in Equation 7 are of little significance since an order of magnitude shift would change the position of the transitions by only some 5 MPa.

A correlation between the type II to III transition and uniaxial yield stress has been reported [18, 19] for a diverse range of 828/TETA systems with the transition occurring at 110 ± 10 MPa. Since only one system was investigated, yield stress may have been an equally good parameter as the minimum post-yield stress.

There is some evidence that the high toughness values associated with type IA fracture are due to plane stress conditions. This will be discussed further in the subsequent paper.

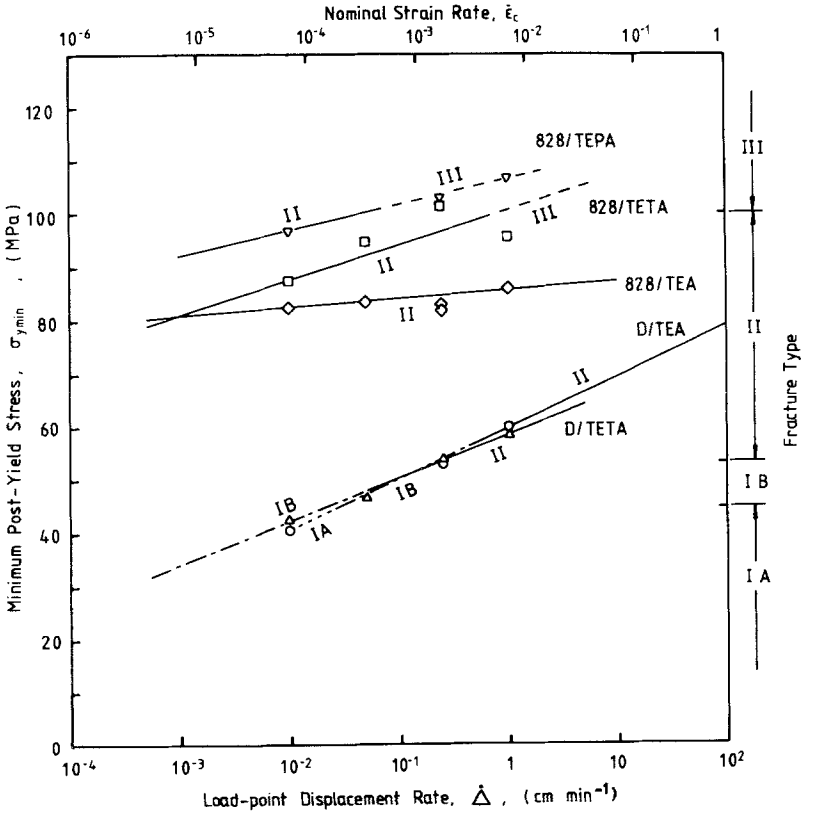

Figure 14 Fracture behaviour, variation with testing rate and strain rate.

6. Conclusions

Fracture in epoxy resins may proceed either by slow stable, fast unstable or fast stable crack growth. The type of fracture behaviour which occurs correlates with the minimum post-yield stress better than with the yield stress. Some evidence for hydrostatic pressure dependence of the yield stress was found for one resin system.

References

1. E. H. ANDREWS and A. STEVENSON, *J. Mater. Sci.* **13** (1978) 1680.
2. R. A. GLEDHILL and A. J. KINLOCH, *Polymer* **17** (1976) 727.
3. R. A. GLEDHILL, A. J. KINLOCH, S. YAMINI and R. J. YOUNG, *ibid.* **19** (1978) 574.
4. J. O. OUTWATER and D. J. GERRY, *J. Adhesion* **1** (1969) 290.
5. D. C. PHILLIPS, J. M. SCOTT and M. JONES, *J. Mater. Sci.* **13** (1978) 311.
6. Y. W. MAI and A. G. ATKINS, *ibid.* **10** (1975) 2000.
7. R. A. GLEDHILL and A. J. KINLOCH, *ibid.* **10** (1975) 1261.
8. D. C. PHILLIPS and J. M. SCOTT, *ibid.* **9** (1974) 1202.
9. S. MOSTOVOY and E. J. RIPLING, *J. Appl. Polymer Sci.* **10** (1966) 1351.
10. *Idem, ibid.* **15** (1971) 641.
11. F. LOHSE, R. SCHMID, H. BATZER and W. FISCH, *Brit. Polymer J.* **1** (1969) 110.
12. A. T. DIBENEDETTO and A. D. WAMBACH, *Int. J. Polymer Mater.* **1** (1972) 159.
13. B. E. NELSON and D. T. TURNER, *J. Polymer Sci. A2* **11** (1973) 1949.
14. S. YAMINI and R. J. YOUNG, *Polymer* **18** (1977) 1075.
15. J. M. SCOTT, G. M. WELLS and D. C. PHILLIPS, *J. Mater. Sci.* **15** (1980) 1436.
16. S. YAMINI and R. J. YOUNG, *ibid.* **14** (1979) 1609.
17. R. J. YOUNG and P. W. R. BEAUMONT, *ibid.* **11** (1976) 776.
18. A. J. KINLOCH and J. G. WILLIAMS, *ibid.* **15** (1980) 987.
19. S. YAMINI and R. J. YOUNG, *ibid.* **15** (1980) 1823.
20. B. W. CHERRY and K. W. THOMSON, *ibid.* **14** (1979) 3004.
21. *Idem, Int. J. Fract.* **14** (1978) R17.
22. C. GURNEY and Y. W. MAI, *Eng. Fract. Mechs.* **4** (1972) 853.
23. Y. W. MAI, *Int. J. Fract.* **10** (1974) 292.
24. M. I. HAKEEM and M. G. PHILLIPS, *J. Mater. Sci.* **13** (1978) 2284.
25. G. P. MARSHALL, L. H. COUTTS and J. G. WILLIAMS, *ibid.* **9** (1974) 1409.
26. S. YAMINI and R. J. YOUNG, *ibid.* **13** (1978) 2287.
27. S. C. MISRA, J. A. MANSON and L. H. SPERLING, in "Epoxy Resin Chemistry", edited by R. S. Bauer, ACS Symposium Series No. 114, (ACS, Washington, 1979), p. 137.
28. R. A. FAVA, *Polymer* **9** (1967) 137.
29. P. B. BOWDEN and J. A. JUKES, *J. Mater. Sci.* **7** (1972) 52.
30. J. G. WILLIAMS and H. FORD, *J. Mech. Eng. Sci.* **6** (1964) 405.
31. T. T. SHIH and J. OPOKU, *Eng. Fract. Mech.* **12** (1979) 479.
32. R. RAGHAVA, R. M. CADDELL and G. S. Y. YEH, *J. Mater. Sci.* **8** (1973) 225.
33. M. J. OWEN and R. G. ROSE, *J. Phys. D.: Appl. Phys.* **6** (1973) 42.
34. G. R. IRWIN, *Appl. Mat. Res.* **3** (1964) 65.

Received 28 February 1980 and accepted 7 January 1981.